CHRONIC OSCILLATORY CHANGE IN DEEP BRAIN STIMULATION FOR DEPRESSION

A PREPRINT

Vineet R. Tiruvadi[*], Sam James[†], Ashan Veerakumar[‡], Andrea Crowell[§], Patricio Riva-Posse[¶], Robert Gross[‖], Cameron McIntyre[**], Helen D. Mayberg[††], Robert Butera[‡‡]

December 17, 2019

ABSTRACT

Deep brain stimulation (DBS) of the subcallosal cingulate cortex white matter (SCCwm) has been shown to alleviated symptoms of treatment resistant depression (TRD). Identifying neural activity that can be used to assess the severity of depression symptoms would enable objective monitoring of treatment response and systematic adjustment of stimulation parameters. Here, we use a novel DBS device capable of simultaneously stimulating and recording to identify oscillations that change in the SCC over six months of treatment. Due to technical limitations shared by all differentially recorded local field potentials (dLFPs), we develop, validate, and implement a cleaning pipeline that enables further analysis. We identify several oscillations that change over the treatment timecourse, primarily in the right SCC-LFP. This work provides an open-source cleaning pipeline for chronic LFP readout identification and a chronic oscillatory readout of depression.

***K*eywords** Deep brain stimulation · Depression · Impedance mismatch · Mismatch compression

1 Introduction

Metabolic activity in the subcallosal cingulate cortex (SCC) is positively correlated with depression severity []. Deep brain stimulation (DBS) in the subcallosal cingulate (SCC) has been shown to alleviate symptoms of TRD. Current implementation and management of DBS relies on clinical assessment depression to assess treatment efficacy and inform stimulation parameter adjustments, which can lead to confounding variability across studies []. Efforts to *close-the-loop* using objective, physiologically derived readouts of depression are growing rapidly []. Electrophysiological correlates of the metabolic state of SCC may contain important information about the depression state if measured over the weeks and months of recovery.

Recording neural activity in clinical patients is difficult, especially in the presence of stimulation artifact. Reliably identifying oscillatory changes in chronic dLFP requires proper accounting of stimulation-artifact related distortions. Electrode impedances can affect the recorded signal and mismatches in a differentially recording channel can result in incomplete rejection of stimulation artifact. In order to accurately assess oscillatory changes, the effects of *mismatch compression* must be accounted for.

[*]Use footnote for providing further
[†]
[‡]
[§]
[¶]
[‖]
[**]
[††]
[‡‡]Use footnote for providing further

In this report we identify oscillatory changes that track with depression recovery after accounting for confounding distortions caused by mismatch compression. First, we demonstrate that mismatch compression is a problem in chronic LFP recordings before developing a strategy to account for them. We then use this strategy in a novel set of clinical LFP recordings to identify oscillations that change significantly over the first six months of DBS therapy. Our results are a putative set of oscillatory readouts that can be used as a feedback signal for adaptive DBS applications. Additionally, this work enables more reliable identification of oscillatory disease readouts in a growing class of aDBS devices that use differentially recorded channels.

2 Methods

2.1 Patients, regulatory, and clinical

Six patients with severe, chronic treatment resistant depression were consented and enrolled in an IRB and FDA approved research protocol at Emory University (clinicaltrials.gov NCT01984710; FDA IDE G130107). Individualized connectome implantation targeting subcallosal cingulate (SCC) white matter was performed as previously described [**?**]. Medtronic 3387 DBS leads with four electrodes, center spacing 3mm apart, were connected to a prototype Activa PC+S™implantable pulse generator (IPG) []. Impedance measurements and depression scales were measured weekly clinical visits. Chronic LFP recordings were downloaded from the DBS IPG during these measurements.

2.2 Depression Scales

Measurement of the severity of depression is done using clinically administered scales []. The Hamilton Depression Rating Scale (HDRS) is a 17-question scale administered to the patient that asks about the presence of depression-related symptoms over the last seven days. We use the HDRS17 score as a scalar measure of weekly depression state. Baseline HDRS17 is determined by averaging the four weeks before DBS implantation. Response is defined as a reduction in the HDRS17 below half of the baseline HDRS17 after six months of DBS therapy (seven months post-implantation). The first week of active DBS therapy is labeled 'C01' and the six month timepoint is labeled 'C24'. In this study we compare oscillatory activity between the C01 and C24 timepoints.

2.3 Electrophysiology

2.3.1 Clinical local field potentials

The Activa PC+S™measured local field potentials *differentially* (dLFP) using the two DBS electrodes immediately adjacent to the stimulation electrode []. This is done to eliminate the stimulation artifact.

The Activa PC+S™is capable of capturing and storing recordings at fixed intervals for later download. Recordings are sampled at 422Hz with a hardware bandpass filter of 0.5Hz and 100Hz. Here, two channels are collected, one each from SCC lead. dLFPs are captured using the two electrodes directly adjacent to the stimulation electrode to maximize symmetric sensing and stimulation filtering (Figure **??**a).

Electrode impedances were measured on all four electrodes for each implanted lead at every clinical assessment across seven months of the study. The standard clinician-controlled Medtronic N'Vision was used to measure impedance in monopolar mode at 3V [**?**].

2.3.2 Benchtop local field potentials

Agar-saline benchtop preparations were created to assess recording fidelity under fixed resistivity differences in media surrounding the DBS lead [**?**]. Saline phase was created with 0.5 mg/mL of NaCl. Two configurations were testing with two agar phase preparations: a high resistivity (0.1 mg/mL of NaCl) yielding impedances of approximately $1300\,\Omega$ and a low resistivity (1mg/mL) yielding impedances of approximately $400\,\Omega$. Agar mixtures was poured into a 10mL conical corning tube and blue fluorophore was added before being placed in a 32C for 20 minutes. Saline phase was then added before DBS3387 lead insertion. A micromanipulator was used to insert and maintain lead location at either uniform saline or agar-saline interface. A single DBS lead was connected to the channels 0-7 on a demo PC+S™unit and recordings were collected using the standard clinical sensing tablet. Impedances were measured using the N'Vision clinician programmer.

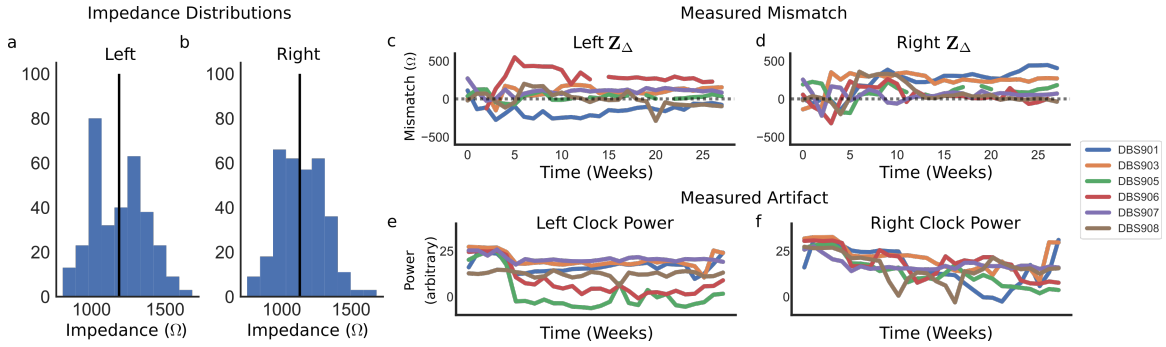

Figure 1: **Recording environment instabilities** a, Impedances in the recording electrodes of all patients demonstrate significant, dynamic mismatches. b, Constant clock signals in recordings demonstrated variability across chronic recordings, suggesting the presence of gain compression.

2.4 Data Analysis

2.4.1 Oscillatory state

Recordings were transformed into the frequency-domain using a Welch power spectral density (PSD) estimate with 1024 FFT bins, 0% overlap, 844 sample Blackman-Harris Windows. PSDs were log-transformed $10 \cdot log_{10}(P_{xx})$ to visualize logPSD and perform preprocessing. Oscillatory power was then computed as either the mean or median value of the PSD for a predefined frequency range corresponding to standard oscillatory bands: δ (1-4Hz), θ (4-8Hz), α (8-14Hz), β (14-30Hz), γ (30-50Hz). Adjusted oscillatory band windows were used to avoid distortions. Polynomial curves were fit to the logPSDs. Power in the 31-33Hz and 63-65Hz range was computed as a measure of gain compression distortion.

2.4.2 Readout identification

To identify candidate oscillatory readouts we perform multiple hypothesis tests across all available oscillations. Two complementary approaches are taken to account for experimental limitations. First, we compare oscillatory recordings between the beginning (C01) and end (C24) of the study for all patients. Second, we compare oscillations between the highest and lowest HDRS17 scores for each patient.

A Kolmogorov-Smirnov test is used to determine whether the oscillatory powers in both weeks are drawn from the same underlying distribution. The KS test is a nonparametric test that was chosen because of the non-normal distribution of the oscillations within each week. A p-value cutoff of $p = 0.005 = \frac{0.05}{10}$ is chosen after a Bonferroni correction for the 10 features being tested.

3 Results

3.1 Instabilities in recording

Over the study timecourse we observed large, dynamic changes in the impedance mismatch across DBS leads and patients (Figure**??**). The dynamics can be divided into three regimes based on their week-to-week variation. First, the highly dynamic regime occurs in the first four weeks following implantation. Second, the early-therapeutic regime occurs in the 10 weeks following initiation of therapeutic stimulation. Finally, the late-therapeutic regime occurs after 10 weeks. This period is characterized by week-to-week stability but, in some cases, non-trivial impedance mismatches.

Characterization of recording stability can be done by assessing the power in the over-range marker over the course of 28 weeks. The over-range marker is a fixed amplitude artifact present in the PC+S hardware (Figure**??**). Variations in the power of this fixed amplitude artifact are ascribed to amplifier gain compression, with saturation being an extreme instance (Supplementary Figure**??**). We observed changes in over-range marker power for all patients across the 28 weeks of study, including the 24 weeks of therapy (Figure **??**d).

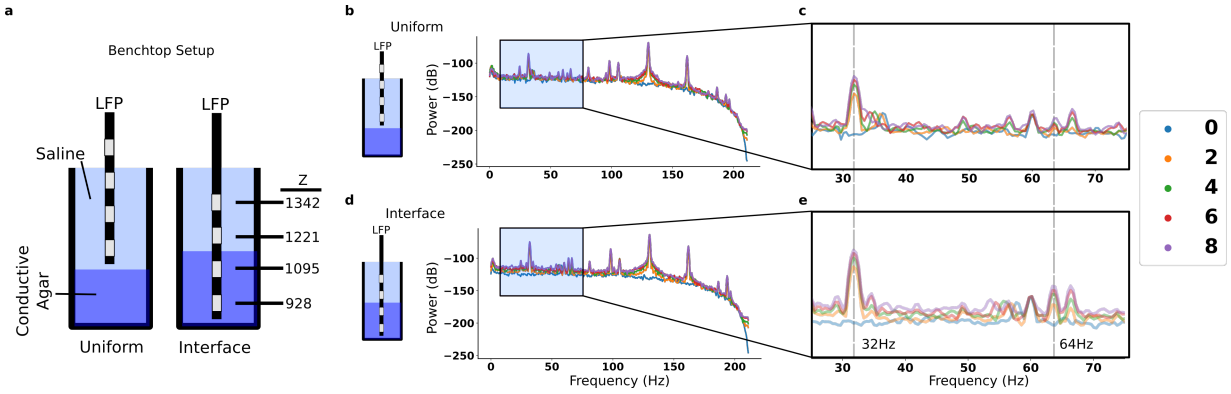

Figure 2: **Benchtop confirmation of mismatch compression** a, A saline-agar construct was created to implement resistivity mismatch. dLFP recordings were captured in two configurations: uniform and interface. Measured impedances ranged between 928 Ω and 1342 Ω. b, Recordings taken uniformly in saline had a mismatch of 120 Ω and demonstrated minimal voltage-dependent PSD changes. Mean PSDs calculated across 20 seconds of active stimulation demonstrate small changes during active stimulation. The larger the stimulation voltage the larger the changes. c, Zoom-in on the 30-70Hz range demonstrates a large 32 Hz artifact and small 64 Hz artifact. d,e Recordings taken at the agar-saline interface had a mismatch of 300 Ω and demonstrated large voltage-dependent PSD changes. The 64 Hz artifact is much larger and noticeably voltage-dependent.

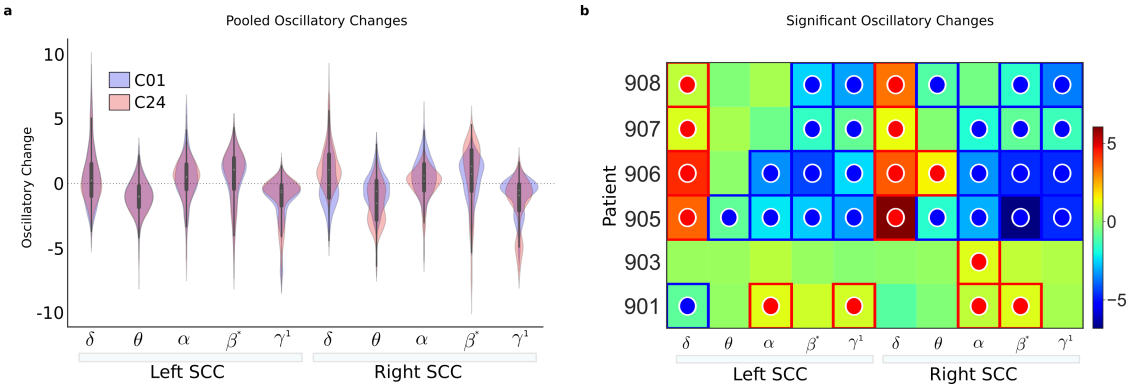

Figure 3: **Oscillatory changes between study beginning and end** a,

3.2 Differences in surrounding media induce gain compression

Recordings were captured with the PC+S™device under variable resistivities. In pure saline (Figure2a) the measured impedance mismatch was 10 Ω. When measured at the interface (Figure2b) the measured impedance mismatch was 100 Ω.

3.3 Oscillations change significantly over study timecourse

Pooled Distributions Oscillatory states differ significantly between the beginning and end of the study (Figure**??**). Statistically significant changes in power occur primarily in right-sided oscillations.

Per-patient Oscillatory changes between C01 and C24 are quantified within each patient (Figure**??**). Oscillations that were significantly different across at least five of the analysed patients were the left β, right θ, right α, and right β ($p<0.005$; Kolmogorov-Smirnov Test, Bonferroni Corrected). The direction of oscillatory change was variable between patients.

4 Discussion

Identifying oscillatory changes in the subcallosal cingulate local field potential may enable objective monitoring, assessment, and management of DBS for depression. In this study we use a novel clinical dataset to identify significant oscillatory changes that occur across SCCwm-DBS treatment. We identify particular oscillatory activity, primarily in the right SCC-LFP, that changes over the timecourse of therapy.

Funding Sources

NIH R01 MH106173, NIH BRAIN UH3NS103550, and the Hope for Depression Research Foundation and The DBS Activa PC+S research devices were donated by Medtronic (Minneapolis, MN).

Conflicts of Interest

Cameron McIntyre is a paid consultant for Boston Scientific Neuromodulation, receives royalties from Neuros Medical and Qr8, and is a shareholder in the following companies: Surgical Information Sciences, Autonomic Technologies, Cardionomic, Enspire DBS. Helen Mayberg has a consulting agreement with Abbott Labs (previously St Jude Medical, Neuromodulation), which has licensed her intellectual property to develop SCC DBS for the treatment of severe depression (US 2005/0033379A1). The terms of this arrangement have been approved by Emory University and Icahn School of Medicine in accordance with policies to manage conflict of interest. All other authors have no COI to declare. Robert Gross serves as a consultant to Medtronic, which manufactures products related to the research described in this paper. Gross receives compensation for these services. The terms of this arrangement have been reviewed and approved by Emory University in accordance with its conflict of interest policies.

Acknowledgements

Thanks to Scott Stanslaski at Medtronic for technical assistance with the Activa PC+S™device. Thank you to members of the Butera Lab that assisted in various facets of this work, particularly Riley Zeller-Townshend, Nathan Kirkpatrick, Patrick Howard. Thank you to Mosadoluwa Obatusin and Sankar Alagappan for reviewing manuscript drafts. Thank you to Dr. Warren Grill for discussions and guidance in study design. Thank you to the clinical team, particularly Sinead Quinn, Lydia Denison, and Dr. Allison Waters.

5 Supplementary

5.1 dLFP Model

We provide a mathematical model that simulates mismatch compression and the distortions it introduces into recordings. This model applies to all differentially-recorded LFP signals and is provided as a simulator to help analyse such signals. While certain PC+S™artifacts are simulated ($105.5\,\mathrm{Hz}$ clock signal), the model is designed to be generalizable for mismatch compression and not device-specific artifacts.

5.1.1 Differential recording

Benchtop experiments with the PC+S™platform confirmed the causal link between impedance mismatch and gain compression. DBS3387 leads were placed in a agar-saline preparation with controlled resistivities in each phase which yielded measurably different impedances (Figure **??**). A voltage sweep experiment was performed in uniform saline and at the interface of saline and low resistance agar (Figure **??**a). Spectrograms visualize the dLFP under both lead placements and exhibit slight variations that are difficult to differentiate visually (Figure **??**b). Oscillatory analyses were then performed to compare PSD of recordings taken at different stimulation voltages (Figure **??**). These observations were consistent with our hypothesis that impedance mismatches cause distortions.

We developed a simplified mathematical model of dLFP recordings to determine whether gain compression was a plausible explanation of distortions. Details are presented below and in Figure **??**.

We modeled three neural oscillatory sources x_1, x_2, and x_3. For this study only x_1 was non-zero. A stationary $15\,\mathrm{Hz}$ sinusoid was used as our neural signal of interest. An independent, stationary $\frac{1}{f}$ brain signal is added to each source. Finally, stimulation artifact is introduced as a truncated Fourier series of sine waves at the therapeutic stimulation

frequency f_T. The series was truncated at three sine waves after visual inspection of the PC+S recorded stimulation and comparison to the true waveform [**?**].

$$S(t) = V_{\text{stim}}(sin(2\pi 130t) + sin(2\pi 260t) + \frac{1}{3}sin(2\pi 390t)) \tag{1}$$

The recording electrodes e_1 and e_3 measure the oscillatory neural sources, a $\frac{1}{f}$ background signal, and the stimulation artifact through independent resistors corresponding to the measured electrode impedances Z_1 and Z_3.

The differential amplifier then outputs the differential signal to the signal amplifier.

$$V_{\text{out}} = A_d Z_b \left(\frac{x_1(t) + \frac{x_2(t)}{c_{12}} + S(t)}{Z_1 + Z_b} - \frac{x_3(t) + \frac{x_2(t)}{c_{32}} + S(t)}{Z_3 + Z_b} \right) \tag{2}$$

In this study, our focus is on the stimulation artifact, specifically the amount that leaks into the differential mode and gets amplified. Hence, we focus on just one part of the output:

$$V_{\text{out}} = A_d Z_b S(t) \left(\frac{1}{Z_1 + Z_b} - \frac{1}{Z_3 + Z_b} \right) \tag{3}$$

5.1.2 Amplifier gain compression

The signal amplifier is modeled in one of three ways. First, a perfect linear amplifier. Second, a piecewise linear amplifier that is linear until it reaches a hard cutoff. Third, a hyperbolic tangent function that has a soft cutoff.

Recording amplifiers exhibit a phenomenon called *gain compression*. This occurs when the input signal goes beyond the design specifications of the amplifier. As an illustration, we model three amplifiers (Figure**??**). We see that the perfect amplifier gains an input signal at a fixed value regardless of the input amplitude. This perfect amplifier is not realizable as all amplifiers have a maximum achievable output voltage.

An amplifier model that is implicitly assumed for clinical recordings is found in Figure**??**b. In this model, the amplifier is perfect up until it reaches its minimum/maximum voltage, or *rails*. This model would exhibit *hard-clipping* which is often mistakenly considered to be the only form of *saturation*.

The most realistic amplifier model is the $tanh(x)$. model in Figure**??**c. Here, the amplifier gradually fails to gain the signal to specifications.

To determine whether gain compression was a plausible explanation of our distortions, we simulated several amplifier models. A perfect amplifier was compared with two realistic amplifier models: hard-clipping and soft-clipping (Figure **??**a). Simulated LFPs are inputs into a modeled differentially recording device under both no stimulation and stimulation (Figure **??**b). The resulting PSD of the simulated output demonstrates the predicted emergence of artifactual peaks, called *intermodulation harmonics* and broad-spectrum *slope flattening* (Figure **??**c). The location of the intermodulation harmonics is predicted and matches up with voltage-sensitive peaks in saline recordings (Figure **??**d). The model predicts the center frequency of intermodulation harmonics when compared to saline recordings and qualitatively reflects the broadband distortions. Intermodulation harmonics occur at integer multiples of 32 Hz under 130Hz stimulation. We observe that the strength of the 64Hz artifact is sensitive to the difference between 8V and 2V stimulation. The hard-clipping and soft-clipping models are sufficient to elicit distortions that are not present under the idealized model.

$$V_{\text{lfp}} = g_2 \cdot \tanh(g_1 \cdot V_{\text{out}}) \tag{4}$$

The output of the signal amplifier is the simulated LFP *recording* of a known simulated LFP from neural sources. The output is analysed using the same tools used for empirical LFP recordings. This model is implemented as a Jupyter Notebook frontend. Both are made available at github.com/virati/LFP_Sim.

Model parameters were chosen to match up visually with empirical PSDs and spectrograms at a Z_δ of $100\,\Omega$.

Figure 4: Caption

5.2 dLFP Simulator Library

The above model of mismatch compression is implemented as an open-source simulator library []. The above model is implemented in a Python library with an interactive Jupyter notebook front-end available as a GitHub repository: https://github.com/virati/dLFP

A Python library was created to mathematically model a generalized bdDBS device that records dLFP. Simulated LFPs with fixed oscillations are sent through an idealized differential amplifier at varying levels of realistic stimulation [**?**] and impedance mismatch. The resulting signal is sent through signal amplifier models corresponding to varying levels of realism to yield a simulated recording. We then used standard analytical approaches to identify oscillatory power in simulated LFP. The model is used to predict the frequencies of gain compression related distortion for any given stimulation frequency, hypothesized oscillations, and impedance mismatches. Model implementation and an interactive Jupyter notebook are available as Supplemental Materials.

5.3 Mitigation Strategy

A conservative strategy is taken to correct for mismatch compression. First, oscillatory band windows are adjusted around intermodulation harmonics that arise from gain compression in the presence of $130\,\mathrm{Hz}$ stimulation. Second, the median oscillatory power is calculated as a surrogate for the power within a band. This avoids the distorting effects of narrowband peaks. Third, polynomial subtraction is done on the broad-spectrum PSD activity to remove. Finally, gain compression is quantified through the ratio of two major intermodulation harmonics as a final check for whether recordings are unsalvagable.

5.3.1 Adjusted Oscillatory Bands

We propose a strategy to mitigate distortions and implement it as a preprocessing pripeline (Figure **??**a). The correction pipeline consists of subtracting a fit polynomial from the log-transformed PSD [**?**], and relying on median calculations of power in gain-compression adjusted oscillatory band windows. We validated the pipeline in the agar-saline voltage sweep dataset (Section 5.1.1) and demonstrated its ability to ignore distortions (Figure **??**).

Additional technical details, including those specific to the Activa PC+S™, follow. First, we suggest a median-based power calculation instead of area under the curve in order to minimize the influence of narrow-band artifacts. The impact of this step is most apparent when applied to the standard oscillatory band powers (Figure **??**c, left). Oscillatory powers under 8V and $0\,\mathrm{V}$ should be identical since there are no neural sources. Median calculations move accurately capture the γ power measured under $0\,\mathrm{V}$ due to the median's robustness to narrowband peaks.

Second, adjustment of oscillatory bands around the intermodulation harmonics results in reduced artifacts in oscillatory power (Figure **??**b, inset). The adjusted bands are as follows: δ (1-4Hz), θ (4-8Hz), α (8-14Hz), β^* (14-25Hz), γ^1 (35-50Hz). β^* adjustments are made empirically to avoid a peak in 27Hz, though this peak is not explained by gain compression distortions. When mean and median powers are calculated with the adjusted bands the measured oscillatory powers are closer to the $0\,\mathrm{V}$ condition (Figure **??**c,right). The adjustments to band power presented here are specific to 130Hz stimulation, however, and appropriate adjustments for different stimulation frequencies can be derived from the provided code library.

Third, polynomial subtraction from the logPSD has been used to identify oscillatory activity and eliminates broadband activity that is corrupted by gain compression. The order of the fit polynomial was based from prior literature [**?**] but adjusted to be a polynomial of o=4. The polynomial curve is fit to a recording's logPSD (Figure **??**b) and subtracted (Figure **??**d). These corrections, when applied to agar-saline recordings at various stimulation voltages (Figure **??**e,g), bring the calculated oscillatory powers together to match the 0V condition (Figure **??**f,h).

Finally, we propose an indirect measure of impedances through the ratio of 32Hz and 64Hz. We find that the ratio increases non-linearly with increasing stimulation voltage (Figure **??**c). This effect is stronger when measuring at the interface for a given stimulation voltage. As a preprocessing step, a study-specific threshold can be defined to remove recordings that are above a certain ratio.

5.4 Uncorrected Analyses

Identical analysis performed on mismatch uncorrected recordings demonstrates major issues. The distribution of oscillatory power between the C01 and C24 weeks demonstrates increased multimodality between patients (FigureS**??**).

References

[1] George Kour and Raid Saabne. Real-time segmentation of on-line handwritten arabic script. In *Frontiers in Handwriting Recognition (ICFHR), 2014 14th International Conference on*, pages 417–422. IEEE, 2014.

[2] George Kour and Raid Saabne. Fast classification of handwritten on-line arabic characters. In *Soft Computing and Pattern Recognition (SoCPaR), 2014 6th International Conference of*, pages 312–318. IEEE, 2014.

[3] Guy Hadash, Einat Kermany, Boaz Carmeli, Ofer Lavi, George Kour, and Alon Jacovi. Estimate and replace: A novel approach to integrating deep neural networks with existing applications. *arXiv preprint arXiv:1804.09028*, 2018.

A_d	Z_b	$\frac{1}{f}$ Strength	x_i amplitude	g_1	g_2
250	$1 \cdot 10^4 \Omega$	$1 \cdot 10^{-3}$	$2 \cdot 10^{-3}$	1	1

Table 1: **Model parameters for qualitative assessment of gain compression**